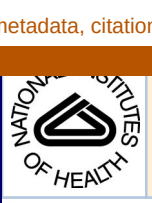

Published in final edited form as:

Exp Cell Res. 2014 February 15; 321(2): 109–122. doi:10.1016/j.yexcr.2013.11.023.

The Regulation of RhoA at Focal Adhesions by StarD13 is Important for Astrocytoma Cell Motility

Bassem D. Khalil[1], **Samer Hanna**[1], **Bechara A. Saykali**[1], **Sally El-Sitt**[1], **Anita Nasrallah**[1], **Daniel Marston**[3], **Marwan El-Sabban**[2], **Klaus M. Hahn**[3], **Marc Symons**[4], and **Mirvat El-Sibai**[1,*]

[1]Department of Natural Sciences, The Lebanese American University, Beirut 1102 2801, Lebanon

[2]Department of Human Morphology, Faculty of Medicine, The American University of Beirut, Beirut, Lebanon

[3]Pharmacology, University of North Carolina School of Medicine CB7365, Chapel Hill, NC27599, USA

[4]Center for Oncology and Cell Biology, The Feinstein Institute for Medical Research at North Shore-LIJ, North Shore University Hospital, Manhasset, NY 11030, USA

Abstract

Malignant astrocytomas are highly invasive into adjacent and distant regions of the normal brain. Rho GTPases are small monomeric G proteins that play important roles in cytoskeleton rearrangement, cell motility, and tumor invasion. In the present study, we show that the knock down of StarD13, a GTPase activating protein (GAP) for RhoA and Cdc42, inhibits astrocytoma cell migration through modulating focal adhesion dynamics and cell adhesion. This effect is mediated by the resulting constitutive activation of RhoA and the subsequent indirect inhibition of Rac. Using Total Internal Reflection Fluorescence (TIRF)-based Förster Resonance Energy Transfer (FRET), we show that RhoA activity localizes with focal adhesions at the basal surface of astrocytoma cells. Moreover, the knock down of StarD13 inhibits the cycling of RhoA activation at the rear edge of cells, which makes them defective in retracting their tail. This study highlights the importance of the regulation of RhoA activity in focal adhesions of astrocytoma cells and establishes StarD13 as a GAP playing a major role in this process.

Keywords

StarD13; RhoA; Rac; Astrocytoma; Cell motility

*Corresponding author: Mirvat El-Sibai, Assistant Professor, Department of Natural Sciences, Lebanese American University, P.O. Box: 13-5053., Chouran 1102 2801, Beirut, Lebanon, Phone: +961-1-786456, ext 1253; Fax: +961-1-867098, mirvat.elsibai@lau.edu.lb.

Introduction

Gliomas, which are neuroepithelial brain tumors derived from astrocytes, oligodendrocytes, or ependymal cells, constitute up to 80% of primary brain tumors in humans [1, 2]. Astrocytomas are gliomas that arise from astrocytes [1]. Malignant astrocytomas are usually associated with poor prognosis and high mortality rate[3]. Malignant astrocytomas rarely metastasize to other organs, but are highly invasive within the brain and could spread to distant regions of the brain, which renders them surgically unmanageable and accounts for their often fatal outcome [4].

Invasion of glioma is a complex process consisting of several steps that involve coordinated intracellular and extracellular interactions [4, 5]. Cell migration is an integral element of the invasion process [4, 5]. To actively migrate, a cell follows a well-defined motility cycle that is initiated in response to the detection of a chemoattractant. This commits the cell to undergo actin polymerization transients in order to extend an actin-rich protrusion, such as lamellipodia or filopodia, towards the direction of the chemoattractant [6]. The steps that follow to achieve the motility cycle include formation of adhesion structures that stabilize the protrusion [7], development of contractile force that translocates the cell body forward, release of adhesion structures at the cell rear and finally retraction of the cell towards the direction of motility [8]. These processes are regulated by Rho family of small guanosine triphosphatases (GTPases), which includes key enzymes that play a major role in the reorganization of the actin cytoskeleton [9].

Rho GTPases are small monomeric G proteins of a 20–40 kDa molecular mass, which belong to the Ras superfamily [10]. The three most characterized and studied members of the Rho family are RhoA, Rac1, and Cdc42 [11]. It was initially believed that RhoA, Rac1 and Cdc42 regulate the formation of actin-myosin filaments, lamellipodia and filopodia respectively [12]. However, recent studies taking into consideration the different effects of Rho GTPases in different cell systems and the cross-talk between the signaling pathways regulated by Rho GTPases, have shown that this model is too simplistic. For instance, the role of RhoA during cell motility was initially thought to be restricted to the generation of contractile force and focal adhesion turnover needed for tail retraction; however, it was recently shown that RhoA is active at the cell edge [13, 14], and that this activation might coordinate the Cdc42 and Rac-1 regulation of the actin cytoskeleton [14, 15]. Moreover, in neutrophils, Rac activation was observed in the tail of the cells in addition to the leading edge [16].

Rho GTPases are found in two forms, a GDP-bound inactive and a GTP-bound active form [17]. As Rho GTPases govern a wide range of critical cellular functions, their function is tightly regulated by three classes of proteins, Guanine nucleotide exchange factors (GEFs), GTPase-activating proteins (GAPs), and guanine nucleotide dissociation inhibitors (GDIs). GAPs negatively regulate Rho GTPases by stimulating the intrinsic GTPase activity of Rho GTPases and promoting the formation of the inactive GDP-bound form [18]. StarD13, which is also referred to as START-GAP2 or DLC2, is a Rho GAP that was first described as a tumor suppressor in hepatocellular carcinoma [19]. This Rho-GAP, whose gene is located on the position 13q12.3, specifically inhibits the function of RhoA and Cdc42 and

was demonstrated to inhibit the Rho-mediated assembly of actin stress fibers in cultured cells.

Overexpression of StarD13 is associated with a decrease in cell growth [19]. Cancer-profiling arrays indicated that StarD13 expression is down-regulated in several types of solid tumors including in renal, uterine, gastric, colon, breast, lung, ovarian, and rectal tumors [20]. Furthermore, a Genome-Wide Analysis integrating a paired copy number and gene expression survey on glioblastoma samples concluded that StarD13 is a potential tumor suppressor gene that could be involved in the resistance of this tumor to etoposide [21].

A study that aimed at examining the intracellular localization of StarD13 showed that it is found in focal adhesions and that it is anchored to tensin2, a component of focal adhesions, through a so-called focal adhesion targeting domain made of amino acids 318–472 in the N-terminal region [22]. StarD13 also plays a role in cell migration and attachment, where its silencing was found to enhance the migration and decrease cell attachment in normal vascular endothelial cells [23]. Moreover, StarD13 deficiency plays a role in the metastasis of breast carcinoma into secondary sites. Using quantitative RT-PCR, a significantly low expression of the StarD13 gene was detected in tumor samples taken from primary ductal carcinomas from patients with metastases into a regional lymph node [20].

In this study, we investigate the role of StarD13-mediated RhoA regulation in astrocytoma cell motility. The knockdown of StarD13 surprisingly inhibited astrocytoma cell motility. This was shown to be mediated by the resulting constitutive activation of RhoA. Similar to the effect of constitutive RhoA activation, StarD13 knockdown resulted in larger focal adhesions. Consequently, the cells were unable to detach their tails, which prohibited the completion of the motility cycle. This study highlights the importance of the regulation of RhoA activity in astrocytoma cell motility and establishes StarD13 as the GAP playing a major role in this process.

Materials and Methods

Cell Culture

Human astrocytoma cell lines SF268 and T98G were cultured in DMEM medium supplemented with 10% FBS and 100U penicillin/streptomycin at 37°C and 5% CO_2 in a humidified chamber.

Antibodies and reagents

Goat polyclonal anti-StarD13 antibody was obtained from Santa Cruz Biotechnology. Mouse monoclonal anti-RhoA, mouse monoclonal anti-Rac1, and mouse monoclonal anti-paxillin antibodies were purchased from Upstate biotechnology, Lake Placid, NY. The anti-Cdc42 antibody (Sc-87) was obtained from Santa Cruz Biotechnology. Anti-goat and anti-mouse HRP-conjugated secondary antibodies were obtained from Promega. Fluorescent secondary antibodies (AlexaFluor 488) and Rhodamin Phalloidin were obtained from Invitrogen. The full length GFP-StarD13 construct was a generous gift from Dr. Hitoshi Yagisawa from the University of Hyogo, Japan (Mammalian expression plasmids for GFP fusion proteins, pEGFPSTART-GAP1(wt)) [22]. The RhoA constructs were a generous gift

from Dr. Hideki Yamaguchi and the Cherry-Rac-DA from Dr. Louis Hodgson from the Albert Einstein College of Medicine, New York, USA.

Cell transfection and small interfering RNA

Cells were transfected with 5 μg GFP-StarD13, Dominant active RhoA, dominant active Rac, or control empty GFP alone vectors using Lipfectamine LTX with Plus reagent (Invitrogen) as described by the manufacturer. The experiments were performed 24 hours following transfection. Goat FlexiTube siRNA for StarD13, RhoA, and Rac1 were obtained from Qiagen. The siRNAs used had the following target sequences: StarD13: Oligo 1, 5′-CCCGCAATACGCTCAGTTATA-3′ and Oligo 2, 5′-ATGGCTACATCCCTACTAATA-3′, RhoA: 5′-TTCGGAATGATGAGCACACAA-3′, and Rac1: 5′-ATGCATTTCCTGGAGAATATA-3′. The cells were transfected with the siRNA at a final concentration of 10 nM using HiPerfect (Qiagen) as described by the manufacturer. Control cells were transfected with siRNA sequences targeting GL2 Luciferase (Qiagen). After 72 hours, protein levels in total cell lysates were analyzed by western blotting using the appropriate antibodies or the effect of the corresponding knock down was assayed.

Pull down assays and Western Blots

The pull-down assays were performed using the RhoA/Rac1/Cdc42 Activation Assay Combo Kit (Cell BioLabs) following the manufacturer's instructions. Briefly, cell lysates were incubated with GST-RBD (for Rho pull down) or GST-CRIB (for Rac pull down) for 1 hour at 4 °C with gentle agitation. Then, the samples were centrifuged, and the pellet washed for several times. After the last wash, the pellets were resuspended with sample buffer and boiled for 5 minutes. GTP-RhoA and GTP-Rac were detected by western blotting using anti-RhoA or anti-Rac, respectively. Total RhoA/Rac and Cdc42 were collected prior to the incubation with GST-RBD/GST-CRIB and used as a loading control. All western blots were analyzed by ECL (GE Healthcare) followed by densitometry.

Immunostaining

Cells were plated on cover slips, and the appropriate treatment was applied. Cells were fixed with 4% paraformaldehyde for 10 minutes at 37°C, and permeabilized with 0.5% Triton-X100 for10 minutes at room temperature. To decrease background fluorescence, cells were rinsed with 0.1 M glycine then incubated with 0.1 M glycine for 10 minutes at room temperature. For blocking, cells were incubated 4 times with 1% BSA, 1% FBS in PBS for 5 minutes at room temperature. Samples were stained with primary antibodies for 2 hours and with fluorophore-conjugated secondary antibodies for 2 hours at room temperature. All fluorescent images were taken using a 60x 1.4 NA infinity corrected optics on a Nikon Eclipse microscope supplemented with a computer-driven Roper cooled CCD camera and operated by IPLab Spectrum software (VayTek).

Wound healing and motility assays

Cells were grown to confluence on culture plates and a wound was made in the monolayer with a sterile pipette tip. After wounding, the cells were washed to remove debris and new

low-serum medium (containing 0.5% FBS) was added. Phase-contrast images of the wounded area were taken at 0 and 24 hours after wounding using a 10X objective. Wound widths were measured at 11 different points for each wound, and the average rate of wound closure was calculated in μm/hr. For motility analysis, images of cells moving randomly in serum were collected every 60 seconds for 2 hours using a 20X objective. During imaging, the temperature was controlled using a Nikon heating stage which was set at 37 °C. The medium was buffered using HEPES and overlayed with mineral oil. The speed of cell movement was quantified using the ROI tracker plugin in the ImageJ software, written by Dr. David Entenberg. This was used to calculate the total distance travelled by individual cells. The speed is then calculated by dividing this distance by the time (120 minutes) and reported in μm/min. The speed of at least 15 cells for each condition was calculated. The net distance travelled by the cell was calculated by measuring the distance travelled between the first and the last frames. Both assays were done using infinity corrected optics on a Nikon Eclipse microscope supplemented with a computer-driven Roper cooled CCD camera and operated by IPLab Spectrum software (VayTek).

RhoA FRET biosensor imaging and analysis

SF268 cells were transfected with 1 μg of the RhoA FLARE biosensor, a fluorescence resonance energy transfer (FRET)-based biosensor plasmid described earlier [13]. FRET image sequences were obtained with an automated Olympus IX70 microscope equipped with filter wheels in the excitation and emission light path and coupled to a cooled SensiCam QE CCD camera (Cooke Corp., MI). CFP was excited using a S430/25 filter with a Sutter DG4 illuminator (Sutter Instruments, Novato, CA) and the fluorescence detected with a S470/30 (donor image) or S535/30 (FRET image) emission filter. YFP was imaged with exciter S500/20 and emitter S535/30 (YFP image). In all cases a dual-band dichroic mirror 86002v2bs was used (Chroma Technology Corp., VT). Images were background corrected and the YFP images were thresholded to generate a binary mask with values of 1 within the cell and 0 for the background. The increase in FRET signal due to activation of RhoA was detected by ratioing the FRET image (CFP excitation- YFP emission) to the donor image (CFP excitation- CFP emission). FRET signals were quantified by averaging the mean FRET ratio in cells. For the live FRET movies, the cells were transfected with the RhoA biosensor as described above, and images of the cells moving randomly in serum were taken at a 1 minute time interval for 1 hour. The images from each frame were analyzed as described above. Detailed description of the image analysis process is described in [24].

TIRF imaging of RhoA activity and mCherry-Paxillin

Astrocytoma cells (SF268) were transfected with 500ng of the RhoA biosensor plasmid and 500ng of the mCherry-Paxillin plasmid using Fugene6. Twenty four hours after transfection, cells were plated onto glass coverslips and allowed to attach for a further 24 hrs prior to imaging. During imaging cells were maintained in Ham's F12(K) (Caisson Labs), supplemented with 5% FBS, at 37°C using a heated stage insert (20/20 Technologies). Cells were imaged using an Olympus IX-81 microscope equipped with a 60x 1.45NA PlanApo TIRF objective, multi-line CELLTIRF system (Olympus) and ES Coolsnap CCD camera (Photometrics). CFP and FRET were excited using a 440nm HeCd laser (Kimmon) and

emission detected using ET470/24M and ET535/30M filters, respectively. mCherry was excited using a 594nm Mambo diode laser (Cobolt) and emission detected using an HQ630/40M filter. In all cases a 445/505/580 ET series dichroic mirror was used (filters and dichroics from Chroma). Images were shade corrected and background subtracted using Metamorph software (Molecular Devices). RhoA activity maps were derived by dividing the FRET image by the CFP image. A detailed description of image analysis used here can be found in [24].

Adhesion assay

96-well plates were coated with collagen using Collagen Solution, Type I from rat tail (Sigma) overnight at 37 °C then washed with washing buffer (0.1% BSA in DMEM). The plates were then blocked with 0.5% BSA in DMEM at 37 °C in a CO2 incubator for 1 hour. This was followed by washing the plates and chilling them on ice. Meanwhile, the cells were trypsinized and counted to 4×10^5 cell/ml. 50 µl of cells were added in each well and incubated at 37°C in a CO2 incubator for 30 minutes. The plates were then shaken and washed 3 times. Cells were then fixed with 4% paraformaldehyde at room temperature for 10 minutes, washed, and stained with crystal violet (5 mg/ml in 2% ethanol) for 10 minutes. Following the staining with crystal violet, the plates were washed extensively with water, and left to dry completely. Crystal violet was solubilized by incubating the cells with 2% SDS for 30 minutes. The absorption of the plates was read at 550 nm using a plate reader.

Statistical analysis

All the results reported represent average values from three independent experiments. All error estimates are given as ± SEM. The p-values were calculated using SPSS software by ANOVA or chi-square tests depending on the experiment.

Results

StarD13 knock down inhibits astrocytoma cell motility through modulating focal adhesion dynamics and cell adhesion

In order to investigate the role of StarD13 in motility of astrocytoma cells, we knocked down its expression using siRNA oligonucleotides and confirmed the knock down by western blot (Figure 1A and S1). We then determined the effect of StarD13 knock down on the rate of wound closure in a wound healing assay as well as on individual cell speed and net distance migrated in time lapse assays. The knock down of StarD13 significantly decreased the wound closure rate (Figure 1B and C). Since Oligo 1 showed higher knock down efficiency (Figure 1A and S1) and a more pronounced effect on cell motility in the wound healing assay, we used this siRNA oligonucleotide to knock down the expression of StarD13 in the following experiments. The decrease in cell migration due to StarD13 knock down was successfully rescued by expressing a GFP-StarD13 construct (Figure 1C and S2), which further shows that the inhibition of migration is due to the loss of StarD13 and not to non-specific off-target effects. StarD13 knock down significantly decreased the average speed of individual cells from 0.44 µm/min to 0.24 µm/min and the net distance migrated from 8.5 µm to 3.02 µm (Figure 1D and E; movie S1). Altogether, these results show that the knock down of StarD13 inhibits astrocytoma cell motility. Similar to its previously reported

localization in HeLa cells [22], our results show that StarD13 colocalizes with two focal adhesion markers, paxillin and vinculin, in both T98G and SF268 astrocytoma cell lines (Figure S3). To determine whether the effect of StarD13 knock down on motility is related to its localization to focal adhesions, we examined the focal adhesion phenotype in control and StarD13 knock down by immunostaining for paxillin, a component of focal complexes and focal adhesions [25]. StarD13 knock down cells showed larger and more prominent focal adhesions at the cell edge (Figure 2A) with more than two-fold increase in area of focal adhesions (Figure 2B). StarD13 knock down cells where StarD13 was overexpressed showed both focal complexes and focal adhesions at the cell edge (Figure 2A, upper right panel) indicating that a normal adhesion phenotype is restored. The formation of focal complexes and their subsequent maturation into focal adhesions has been reported to be regulated by Rac and Rho, respectively [25–27]. We confirmed this in astrocytoma cells since the knock down of Rac resulted in cells with no adhesion structures at the cell edge, while cells where RhoA was knocked down showed only small punctate focal complexes (Figure 2A, lower panel). The fact that StarD13 knock down resulted in the formation of large focal adhesions suggested that StarD13 might be important for focal adhesion dynamics in astrocytoma cells. To test this, we performed time lapse analysis on control or StarD13 knock down cells that are transfected with a GFP-tagged construct of vinculin, a component of focal adhesions [25]. While control cells showed dynamic assembly and disassembly of adhesion structures as they migrated, StarD13 knock down cells were static and showed longer-lived stable adhesion structures (Figure 2C and D; movie S2). Many of the StarD13 knock down cells were also unable to detach their tails and move forward as observed in time lapse analysis of randomly migrating cells (Figure 2E; movie S3). Accordingly, cells where StarD13 was knocked down showed more than a two-fold increase in adhesion to collagen matrix (Figure 2F and G).

The effect of StarD13 knock down on cell motility is through RhoA and Rac

StarD13 was described as a GAP for RhoA and Cdc42 but not for Rac [19]. We have previously reported that StarD13 also plays this role in astrocytoma cells through overexpressing StarD13 [28]. In the current study, we performed pull-down assays to determine the level of Rho GTPase activation in StarD13 knock down cells. As expected, the knock down of StarD13 caused a decrease in RhoA activation (Figure 3A). Interestingly, Rac activation was lower in StarD13 knock down cells as compared to control cells (Figure 3A). Based on the antagonistic relationship between RhoA and Rac in these cells as evident by the increase in Rac activation upon RhoA knock down (Figure 3A), we hypothesized that StarD13 could be affecting Rac activation indirectly through its activity on RhoA. This was confirmed since the simultaneous knock down of RhoA and StarD13 prevented the decrease in Rac activation caused by the absence of StarD13 (Figure 3A). This suggested that the effect of StarD13 knock down on cell motility is mediated through the direct increase in RhoA activation, the subsequent decrease in Rac activation, or both. Therefore, we next determined the effect of knocking down Rac as well as expressing a dominant active form of RhoA on astrocytoma cell motility. Knock down of Rac by siRNA as verified by western blot (Figure 3B) inhibited cell motility. In the wound healing assay, Rac1 knock down decreased wound closure rate from 8.22 μm/hr to 1.76 μm/hr (Figure 3C and D). Likewise, there was a significant decrease in cell speed from 0.44 μm/min to 0.17 μm/min and the net

distance migrated from 8.50 μm in controls to 1.7 μm (Figure 3E and F; movie S4). Expression of dominant active RhoA also inhibited cell motility similar to StarD13 knock down. In the wound healing assay, dominant active RhoA decreased wound closure rate from 7 μm/hr to 2.7 μm/hr (Figure 4A and B). Similarly, dominant active RhoA decreased average cell speed from 0.34 μm/min to 0.25 μm/min (Figure 4D; movie S5). A more substantial decrease in the net path was observed in cells transfected with dominant active RhoA from 9.31 μm to 1.43 μm (Figure 4C and D; S5).

To confirm that StarD13 knock down is affecting motility through RhoA and Rac, we expressed dominant active Rac or knocked down RhoA in StarD13 knock down cells (Figure 5A) and determined the effect on cell motility. The decrease in cell motility caused by the absence of StarD13 was completely or partially reversed by the expression of dominant active Rac and the knock down of RhoA, respectively (Figure 5B and C). When both RhoA and Rac were knocked down in StarD13 knock down cells, the motility of cells was almost completely inhibited (Figure 5B and C).

RhoA knockdown or dominant active Rac in StarD13 knockdown cells reverses the stabilization of focal adhesions

To show that constitutive activation of RhoA due to the knock down of StarD13 is leading to the stabilization of focal adhesions, we determined the effect of knocking down RhoA in StarD13 knock down cells on focal adhesions. This led to the abolishment of focal adhesions, where only immature focal complexes were observed (Figure 5D). The expression of a dominant active Rac also led to the absence of the large focal complexes induced by the knockdown of StarD13, where both focal complexes and focal adhesions were observed (Figure 5D). Consistently, the knockdown of both RhoA and Rac in StarD13 knockdown cells led to the complete absence of any form of adhesion (Figure 5D).

StarD13 knock down inhibits the cycling in RhoA activation

The fact that the constitutive increase in RhoA activity either by the knockdown of StarD13 or the expression of a dominant active RhoA is inhibiting motility implies that RhoA has to be inactivated at some point in the cell motility cycle for the cells to move efficiently. To investigate this possibility, we transfected control or StarD13 knock down astrocytoma cells with a RhoA FRET biosensor in order to determine the temporal and spatial dynamics of RhoA activation in cells undergoing random motility. At the cell tail of control cells (identified by a white box in the upper panel of Figure 6A), RhoA showed cycles of activation and inactivation (Figure 6A upper panel and B; movie S6). A decline in RhoA activation was specifically evident as the cell retracted its tail to move forward (time points 16′ and 20′). As previously described, a phenotype that was evident in cells where StarD13 was knocked down is the inability of cells to retract their tail and move forward.. FRET analysis showed that this phenomenon was correlated with a high and persistent RhoA activation at the tail as seen in the StarD13 knock down cells transfected with the RhoA FRET biosensor (Figure 6A lower panel and B; movie S7). We also detected RhoA activation at the edge of cells as well as the tail (Figure S4A). Accordingly we suspected that, other than its effect at the cell tail, StarD13 knock down inhibits cell motility by altering the dynamics of cell adhesions at the cell edge. Indeed, other than its cycles of

activation and inactivation at the tail of cells undergoing motility, RhoA showed cycles of activation and inactivation at the leading edge of cells towards the direction of movement as well (Figure S4B). At the leading edge of protrusions, RhoA activation was more persistent in cells where StarD13 was knocked down (Figure S5). Similar to the previously described effect of dominant active RhoA on inhibition of cell migration, and consistent with the idea that cycling of RhoA activity is required for efficient migration, knock down of RhoA also inhibited cell migration in the wound healing and time lapse assays (Figure S6; movie S8). To show that RhoA is active at the basal surface of cells, where focal adhesions are localized, we performed TIRF-based FRET analysis on cells simultaneously transfected with RhoA FRET biosensor and mCherry-paxillin. These studies showed that RhoA activity is distributed at the basal surface, where high activity colocalizes with adhesive structures (Figure 6C; movie S9). These experiments also confirmed that RhoA activity is distributed along the whole cell edge before the cell starts migrating (Figure 6C left panel).

Discussion

StarD13 is a Rho GAP that inhibits the activity of RhoA and Cdc42. Previous studies have shown its inhibitory effect against RhoA in hepatocellular carcinoma cells [19] and its localization to focal adhesions in HeLa cells [22]. StarD13 was also found to inhibit cell motility in hepatocellular carcinoma which was consistent with its role as a tumor suppressor [29]. However, its role in astrocytoma has never been studied. We recently published a paper showing that StarD13 plays a role of a tumor suppressor in astrocytoma [28]. In the current study, we investigate the role of StarD13 in astrocytoma cell motility. This was highly intriguing given the crucial role of Rho GTPases, the downstream effectors of StarD13, and focal adhesions to which StarD13 localizes in cell motility and tumor invasion. To our surprise, and in contrast to its role as a tumor suppressor, the knock down of StarD13 decreased the migration of astrocytoma cells. In order to confirm the specificity of this effect, we used a second StarD13 siRNA oligonucleotide that also resulted in a similar inhibition in cell motility. In addition, the expression of wild type StarD13 in cells with StarD13 knock down was able to restore cell migration to a level similar to wild type cells. This further confirms that the loss of StarD13 in cells transfected with the StarD13 siRNA is responsible for the decrease in cell motility observed.

Previous reports that investigated the role of StarD13 in cell motility showed that it negatively regulates motility [29, 30]. However, there are no previous reports on the role of StarD13 in astrocytoma or glioblastoma cells. The discrepancy between our results and the previous reports could be due to the fact that the dependence of migration on RhoA-governed adhesion turnover is different in distinct cell types. Indeed, in glioblastoma, the model that we are investigating in the current study, the aberrant increase in RhoA activity has been linked to impaired cell migration through inducing profound morphological changes including the rearrangement of actin into stress fibers and the formation of focal adhesions. These changes, which are mainly linked to RhoA activity, increased the attachment of cells to matrix and rendered them immobile [31]. In fact, there are also contradictory results regarding the role of a closely related protein, DLC1, in cell migration. DLC1 is a well-established tumor suppressor that has been shown to inhibit proliferation, induce apoptosis, and suppress migration [32]. However, at least two reports show that

DLC1 positively regulates cell migration similar to our data with DLC2. In the first report, the proper localization of DLC1 to focal adhesions in HeLa cells has been shown to be necessary for cell migration [33]. The other study recently reported that the silencing of DLC1 in prostate cells significantly inhibits cell migration as determined by wound-healing and transwell assays, which is a result similar to our findings for DLC2 [34] Indeed, in our system, the knock down of StarD13 in HUVEC cells did not result in a significant change in cell motility in a wound healing assay (Figure S7). Interestingly, we have previously reported that the expression of StarD13 is higher in grade IV as compared to grade I human astrocytoma tissues [28]. In the same report, we presented data from REMBRANDT database showing that although the mRNA expression of StarD13 is higher in grade IV human astrocytoma samples as compared to lower grades, it was still lower than the expression in non-tumor tissues. This suggests that, consistent with its tumor suppressor role, an initial decrease in StarD13 levels might contribute to the initiation of astrocytic tumors. However, as the tumor progresses, it accumulates novel mutations that increase StarD13 to adequate levels that would, based on our current data, provide migratory and invasive properties to astrocytoma cells.

In this study as well as in a previous report [28] we showed that StarD13 indeed functions as a GAP for RhoA in astrocytoma cells. We also confirmed that StarD13 localizes to focal adhesions in these cells since it colocalizes with paxillin and vinculin. Hence, we hypothesized that the knock down of StarD13 led to the constitutive activation of RhoA in focal adhesions, which in turn inhibited cell motility. In order to mimic the effect of StarD13 knock down and to determine the effect of the constitutive activation of RhoA on cell motility, we transfected astrocytoma cells with dominant active of RhoA. Indeed, this resulted in decreased cell motility similar to the knock down of StarD13. The decrease in cell motility due to the constitutive activation of RhoA has been reported before in other systems [35–38]. In fact, the correlation of RhoA expression and activity with brain tumor progression and cell motility remains a highly debatable issue in the literature (discussed in [39]). Our results show that the knock down of RhoA using siRNA decreases the motility of cells. A previous study has reported that RhoA is needed for the migration of glioma cells in response to lysophosphatidic acid (LPA), an agent that is able to strongly induce chemokinesis and chemotaxis in human glioma cells [40]. Moreover, the use of RNA interference to deplete mDia1, another downstream effector of Rho, inhibited both adhesion turnover and cell polarization in rat C6 glioma cells, which rendered them unable to undergo directed migration [41]. Indeed, a positive role of RhoA or its downstream effectors in cell motility and invasion has been described in many cell systems [42–46]. On the other hand however, inhibition of the RhoA effector ROCK has been shown to enhance the invasive and migratory properties of glioblastoma cells [47]. Interestingly, we detected a decrease in Rac activation when StarD13 was knocked down, which is consistent with the antagonistic relationship between RhoA and Rac activity we also observed in these cells. Hence, the inhibition of astrocytoma cell motility when StarD13 is knocked down could be secondary to Rac inhibition caused by the constitutive activation of RhoA. To investigate this possibility, we determined the individual effect of Rac knock down on cell motility. The absence of Rac did indeed inhibit cell motility. Importantly, the transfection of StarD13 knock down cells with active Rac was able to completely restore cell motility to normal

levels. The ability of dominant active Rac to restore cell motility could be due to the fact that dominant active Rac is neutralizing the effect of StarD13 knock down on Rac inhibition, which brings back the activation state to normal levels. Collectively, the previously discussed observations suggest that the constitutive activation of RhoA in the absence of StarD13 could be inhibiting cell motility either directly or indirectly through inhibiting Rac or a combination of both.

After verifying that StarD13 localizes to focal adhesions in astrocytoma cells, and in order to determine the mechanism through which StarD13 knock down is inhibiting motility, we started investigating the hypothesis that the knockdown of StarD13 leads to constitutive activation of RhoA in focal adhesions, which leads to the stabilization of focal adhesions by preventing their disassembly and ultimately inhibiting cell migration. A high level of focal adhesions inhibits cell migration because of the strength of attachment to the extracellular matrix [48]. At the tail, RhoA activation in adhesion complexes must be inhibited since tail detachment can often be the rate-limiting step of cell migration [43]. Time-lapse movies of StarD13 knockdown cells showed that a large proportion of cells were unable to move forward due to their inability to retract their tail. This was accompanied by persistent activation of RhoA at the cell tail as revealed by FRET analysis. Hence, StarD13 might be playing a role in the inhibition of RhoA in focal adhesions at the tail of cells, which seems to be an important event for the cells to be able to detach their tails and to pull themselves and move forward. Our results verified this hypothesis, as StarD13 silencing induced the formation of larger and thicker focal adhesions especially at the tail of cells. This was also supported by the fact that cells with StarD13 knock down were more adhesive to collagen than control cells. The increase in adhesion could have prevented the retraction of the tail, which we suspect is the major event that impeded cell motility.

One instance where RhoA could be needed in cell motility is for the stabilization of protrusions through inducing the maturation of focal complexes into focal adhesions, a process that we have shown to be inhibited in the absence of RhoA as previously discussed. Focal complexes are small punctate structures formed behind the front of the lamellipodium [49]. These structures do not confer enough contractility needed for cell motility [49]. Focal complexes are precursors for focal adhesions, which appear larger in size and less persistent [49], and are needed to provide the cell with the mechanical strength needed for the cell body to contract and move forward [7]. However, in order for RhoA to be able to drive the conversion of focal complexes into focal adhesions, Rac must first induce the formation of these focal complexes. This is confirmed by our results that show the absence of both focal complexes and focal adhesions when Rac is knocked down. On the other hand, cells showed exaggerated focal complexes with a complete absence of focal adhesions when RhoA was knocked down. In fibroblasts, it was shown that initial cell spreading is associated with the formation of focal complexes and with high Rac activation [49, 50]. Formation of focal complexes stabilizes the lamellipodium of migrating cells by binding to the ECM [8]. Some studies described a high FAK activation during initial cell spreading, which potentiates Rac1 activation and suppresses RhoA activation [51, 52]. This initial dip in RhoA activity may allow Rac to initiate the formation of focal complexes. This also suggests sequential roles of Rac and RhoA in adhesion, whereby initially RhoA activation is suppressed allowing Rac-dependent focal complex formation and allowing the cells to spread. This is followed by

high RhoA activation which leads to the maturation of focal complexes into focal adhesions. The activation of RhoA possibly leads to the local inhibition of Rac in order to allow the focal complexes to mature. As previously discussed, we did observe an increase in Rac activation when RhoA was knocked down and a decrease in Rac activation when StarD13 was knocked down. It is classically accepted that RhoA and Rac cross-talk and that they tend to have an inverse relationship [53]. A mechanism through which Rac inhibits Rho was proposed, whereby Rac mediates the production of oxygen radicals which causes the phosphorylation and activation of p190 RhoGAP. This, in turn, results in the inactivation of Rho [54]. Recently, it was shown that Rho leads to the inhibition of Rac through the ROCK-dependent Rac GAP, filamin GAP (FilGAP) [55]. Whereas ROCK inhibited Rac, mDia was found to activate Rac in the same cells, independently of ROCK, through the Cas/DOCK180 pathway [41, 56]. The fact that the knock down of RhoA in StarD13 knockdown cells caused the total disappearance of focal adhesions supports the idea that these structures are caused by the constitutive activation of RhoA in the absence of StarD13. It is important to note that no focal adhesions were observed in these cells. The knockdown of RhoA was not able to completely reverse the inhibition in motility caused by the knockdown of StarD13, as normal focal adhesion formation is needed for efficient cell migration. This is consistent with the fact that the knock down of both RhoA and Rac in StarD13 knock down cells completely paralyzed the cells.

Our hypothesis that the knock down of StarD13 is inhibiting cell motility through the constitutive activation of RhoA is also highly reinforced by our results showing that RhoA undergoes cycles of activation and inactivation, and that this cycling is abolished when StarD13 is absent. Spatio-temporal analysis of RhoA activation by time-lapse FRET showed that the cycling of RhoA occurs at both the tail and the leading edge of cells. The inhibition of RhoA at the leading edge of cells is most probably important for the activation of Rac and the subsequent formation of focal contacts. FRET analysis also showed that in the absence of StarD13 there is a persistent high activity of RhoA at the cell tail and the leading edge of cells. Altogether, this data suggests that StarD13 is necessary for the inhibition of RhoA both at the cell tail and at the cell front. These events are required for the tail to retract and Rac to become active and induce the formation of focal complexes, respectively. Then, the activation of RhoA at the cell edge is needed for these focal complexes to mature generating the necessary tension for the cell to move forward. Importantly, through imaging of cells using TIRF-based FRET, we were able to show that RhoA activity colocalizes with focal adhesions at the basal surface of cells.

This paper also shows that RhoA should be activated at the leading edge of astrocytoma cells, as previously established for breast cancer cells [14]. The role of RhoA at the edge is to allow the maturation of Rac-mediated focal complexes into focal adhesions since the absence of RhoA leads to the absence of focal adhesions and the accumulation of focal complexes (this study and [14]. Even though protrusion is unaffected, the absence of focal adhesions leads to an ineffective protrusion with not enough traction force on the ECM for the cells to move forward [7]. In this system and in other systems in previous work [14, 57], we have shown that defective adhesions due to inhibition of Rac or RhoA, though they do not affect protrusion, inhibits cell motility. Hence, as we describe a need to inhibit RhoA at the tail of cells, we also confirm the newly described role of RhoA at the leading edge of

cancer cells undergoing movement, contrary to the canonical distribution of RhoA activation.

This work establishes that, in addition to the activation of RhoA needed for the stabilization of protrusions (at the cell edge) and the generation of contractile force (along the cell body), an equally important event in the cell motility cycle is the inactivation of RhoA in focal adhesions at the cell tail. This is needed for the dissolution of these adhesions and the successful retraction of the tail. This work also defines StarD13, which is probably one member of a whole orchestra of GEFs and GAPs coordinating the activation and inactivation of RhoA respectively, as an important regulator of the cell motility cycle. One GAP that could also be playing such a role is DLC1, which belongs to the same family as StarD13. It would also be intriguing to investigate a possible role for DLC1 in focal adhesion dynamics and spatial regulation of RhoA activation.

Supplementary Material

Refer to Web version on PubMed Central for supplementary material.

Acknowledgments

The authors are very appreciative to Dr. Jonathan Backer's intellectual input and critical reading of the manuscript. The authors would also like to thank Dr. Najla Fakhreddine (from Hammoud hospital, Saida, Lebanon) for her help in providing human brain tumor tissues. We would also like to thank Dr. Noha Bajjani, from Rizk Medical Center. The authors would also like to thank Dr. Omar Itani (Balamand University) for technical assistance and Drs. Hitoshi Yagisawa, Hideki Yamaguchi and Amber Wells for providing constructs. The ROI_Tracker software was supplied by David Entenberg and John Condeelis as supported by CA100324 and GM064346. This work was supported by the Natural Science Department at the Lebanese American University, by the University Research Council (URC) at LAU, by the Lebanese National Center for Scientific Research (L-NCSR)(Ref: 03-06-10) and by the NIH grant GM057464.

References

1. Louis, DN.; Ohgaki, H.; Wiestler, OD.; Cavenee, WK. WHO Classification of Tumours of the Central Nervous System. World Health Organization; 2007.
2. CBTRUS. CBTRUS Statistical Report: Primary Brain and Central Nervous System Tumors Diagnosed in the United States in 2004–2007. Central Brain Tumor Registry of the United States; Hinsdale, IL: 2011.
3. Wen PY, Kesari S. Malignant gliomas in adults. N Engl J Med. 2008; 359:492–507. [PubMed: 18669428]
4. Nakada M, Nakada S, Demuth T, Tran NL, Hoelzinger DB, Berens ME. Molecular targets of glioma invasion. Cell Mol Life Sci. 2007; 64:458–478. [PubMed: 17260089]
5. Giese A, Bjerkvig R, Berens ME, Westphal M. Cost of migration: invasion of malignant gliomas and implications for treatment. J Clin Oncol. 2003; 21:1624–1636. [PubMed: 12697889]
6. Bailly M, Condeelis JS, Segall JE. Chemoattractant-induced lamellipod extension. Microsc Res Tech. 1998; 43:433–443. [PubMed: 9858340]
7. Gupton SL, Waterman-Storer CM. Spatiotemporal feedback between actomyosin and focal-adhesion systems optimizes rapid cell migration. Cell. 2006; 125:1361–1374. [PubMed: 16814721]
8. Condeelis JS, Wyckoff JB, Bailly M, Pestell R, Lawrence D, Backer J, Segall JE. Lamellipodia in invasion. Semin Cancer Biol. 2001; 11:119–128. [PubMed: 11322831]
9. Ridley AJ, Hall A. The small GTP-binding protein rho regulates the assembly of focal adhesions and actin stress fibers in response to growth factors. Cell. 1992; 70:389–399. [PubMed: 1643657]

10. Takai Y, Sasaki T, Matozaki T. Small GTP-binding proteins. Physiol Rev. 2001; 81:153–208. [PubMed: 11152757]
11. Etienne-Manneville S, Hall A. Rho GTPases in cell biology. Nature. 2002; 420:629–635. [PubMed: 12478284]
12. Bishop AL, Hall A. Rho GTPases and their effector proteins. Biochem J. 2000; 348(Pt 2):241–255. [PubMed: 10816416]
13. Pertz O, Hodgson L, Klemke RL, Hahn KM. Spatiotemporal dynamics of RhoA activity in migrating cells. Nature. 2006; 440:1069–1072. [PubMed: 16547516]
14. El-Sibai M, Pertz O, Pang H, Yip SC, Lorenz M, Symons M, Condeelis JS, Hahn KM, Backer JM. RhoA/ROCK-mediated switching between Cdc42- and Rac1-dependent protrusion in MTLn3 carcinoma cells. Exp Cell Res. 2008; 314:1540–1552. [PubMed: 18316075]
15. Machacek M, Hodgson L, Welch C, Elliott H, Pertz O, Nalbant P, Abell A, Johnson GL, Hahn KM, Danuser G. Coordination of Rho GTPase activities during cell protrusion. Nature. 2009; 461:99–103. [PubMed: 19693013]
16. Gardiner EM, Pestonjamasp KN, Bohl BP, Chamberlain C, Hahn KM, Bokoch GM. Spatial and temporal analysis of Rac activation during live neutrophil chemotaxis. Curr Biol. 2002; 12:2029–2034. [PubMed: 12477392]
17. Bourne HR, Sanders DA, McCormick F. The GTPase superfamily: a conserved switch for diverse cell functions. Nature. 1990; 348:125–132. [PubMed: 2122258]
18. Moon SY, Zheng Y. Rho GTPase-activating proteins in cell regulation. Trends Cell Biol. 2003; 13:13–22. [PubMed: 12480336]
19. Ching YP, Wong CM, Chan SF, Leung TH, Ng DC, Jin DY, Ng IO. Deleted in liver cancer (DLC) 2 encodes a RhoGAP protein with growth suppressor function and is underexpressed in hepatocellular carcinoma. The Journal of biological chemistry. 2003; 278:10824–10830. [PubMed: 12531887]
20. Ullmannova V, Popescu NC. Expression profile of the tumor suppressor genes DLC-1 and DLC-2 in solid tumors. Int J Oncol. 2006; 29:1127–1132. [PubMed: 17016643]
21. de Tayrac M, Etcheverry A, Aubry M, Saikali S, Hamlat A, Quillien V, Le Treut A, Galibert MD, Mosser J. Integrative genome-wide analysis reveals a robust genomic glioblastoma signature associated with copy number driving changes in gene expression. Genes Chromosomes Cancer. 2009; 48:55–68. [PubMed: 18828157]
22. Kawai K, Seike J, Iino T, Kiyota M, Iwamae Y, Nishitani H, Yagisawa H. START-GAP2/DLC2 is localized in focal adhesions via its N-terminal region. Biochem Biophys Res Commun. 2009; 380:736–741. [PubMed: 19250640]
23. Lin Y, Chen NT, Shih YP, Liao YC, Xue L, Lo SH. DLC2 modulates angiogenic responses in vascular endothelial cells by regulating cell attachment and migration. Oncogene. 2010; 29:3010–3016. [PubMed: 20208559]
24. Hodgson L, Shen F, Hahn K. Biosensors for characterizing the dynamics of rho family GTPases in living cells. Curr Protoc Cell Biol Chapter. 2010; 14(Unit 14):11, 11–26.
25. Zaidel-Bar R, Cohen M, Addadi L, Geiger B. Hierarchical assembly of cell-matrix adhesion complexes. Biochem Soc Trans. 2004; 32:416–420. [PubMed: 15157150]
26. Nobes CD, Hall A. Rho, rac, and cdc42 GTPases regulate the assembly of multimolecular focal complexes associated with actin stress fibers, lamellipodia, and filopodia. Cell. 1995; 81:53–62. [PubMed: 7536630]
27. Rottner K, Hall A, Small JV. Interplay between Rac and Rho in the control of substrate contact dynamics. Curr Biol. 1999; 9:640–648. [PubMed: 10375527]
28. El-Sitt S, Khalil BD, Hanna S, El-Sabban M, Fakhreddine N, El-Sibai M. DLC2/StarD13 plays a role of a tumor suppressor in astrocytoma. Oncology reports. 2012; 28:511–518. [PubMed: 22614672]
29. Leung TH, Ching YP, Yam JW, Wong CM, Yau TO, Jin DY, Ng IO. Deleted in liver cancer 2 (DLC2) suppresses cell transformation by means of inhibition of RhoA activity. Proceedings of the National Academy of Sciences of the United States of America. 2005; 102:15207–15212. [PubMed: 16217026]

30. Fan Q, He M, Deng X, Wu WK, Zhao L, Tang J, Wen G, Sun X, Liu Y. Derepression of c-Fos caused by MicroRNA-139 down-regulation contributes to the metastasis of human hepatocellular carcinoma. Cell biochemistry and function. 2012
31. Goldberg L, Kloog Y. A Ras inhibitor tilts the balance between Rac and Rho and blocks phosphatidylinositol 3-kinase-dependent glioblastoma cell migration. Cancer research. 2006; 66:11709–11717. [PubMed: 17178866]
32. Lukasik D, Wilczek E, Wasiutynski A, Gornicka B. Deleted in liver cancer protein family in human malignancies (Review). Oncology letters. 2011; 2:763–768. [PubMed: 22866123]
33. Kawai K, Iwamae Y, Yamaga M, Kiyota M, Ishii H, Hirata H, Homma Y, Yagisawa H. Focal adhesion-localization of START-GAP1/DLC1 is essential for cell motility and morphology. Genes Cells. 2009; 14:227–241. [PubMed: 19170769]
34. Shih YP, Takada Y, Lo SH. Silencing of DLC1 upregulates PAI-1 expression and reduces migration in normal prostate cells. Molecular cancer research : MCR. 2012; 10:34–39. [PubMed: 22064653]
35. Banyard J, Anand-Apte B, Symons M, Zetter BR. Motility and invasion are differentially modulated by Rho family GTPases. Oncogene. 2000; 19:580–591. [PubMed: 10698528]
36. Li L, Li J, Wang JY, Yang CQ, Jia ML, Jiang W. Role of RhoA in platelet-derived growth factor-BB-induced migration of rat hepatic stellate cells. Chin Med J (Engl). 2010; 123:2502–2509. [PubMed: 21034618]
37. Tkach V, Bock E, Berezin V. The role of RhoA in the regulation of cell morphology and motility. Cell Motil Cytoskeleton. 2005; 61:21–33. [PubMed: 15776463]
38. Vial E, Sahai E, Marshall CJ. ERK-MAPK signaling coordinately regulates activity of Rac1 and RhoA for tumor cell motility. Cancer Cell. 2003; 4:67–79. [PubMed: 12892714]
39. Khalil BD, El-Sibai M. Rho GTPases in primary brain tumor malignancy and invasion. Journal of neuro-oncology. 2012; 108:333–339. [PubMed: 22528793]
40. Manning TJ Jr, Parker JC, Sontheimer H. Role of lysophosphatidic acid and rho in glioma cell motility. Cell Motil Cytoskeleton. 2000; 45:185–199. [PubMed: 10706774]
41. Yamana N, Arakawa Y, Nishino T, Kurokawa K, Tanji M, Itoh RE, Monypenny J, Ishizaki T, Bito H, Nozaki K, Hashimoto N, Matsuda M, Narumiya S. The Rho-mDia1 pathway regulates cell polarity and focal adhesion turnover in migrating cells through mobilizing Apc and c-Src. Molecular and cellular biology. 2006; 26:6844–6858. [PubMed: 16943426]
42. Hakuma N, Kinoshita I, Shimizu Y, Yamazaki K, Yoshida K, Nishimura M, Dosaka-Akita H. E1AF/PEA3 activates the Rho/Rho-associated kinase pathway to increase the malignancy potential of non-small-cell lung cancer cells. Cancer research. 2005; 65:10776–10782. [PubMed: 16322223]
43. Ridley AJ. Rho GTPases and cell migration. Journal of cell science. 2001; 114:2713–2722. [PubMed: 11683406]
44. Sahai E, Marshall CJ. Differing modes of tumour cell invasion have distinct requirements for Rho/ROCK signalling and extracellular proteolysis. Nature cell biology. 2003; 5:711–719.
45. Takaishi K, Kikuchi A, Kuroda S, Kotani K, Sasaki T, Takai Y. Involvement of rho p21 and its inhibitory GDP/GTP exchange protein (rho GDI) in cell motility. Molecular and cellular biology. 1993; 13:72–79. [PubMed: 8417362]
46. Worthylake RA, Lemoine S, Watson JM, Burridge K. RhoA is required for monocyte tail retraction during transendothelial migration. The Journal of cell biology. 2001; 154:147–160. [PubMed: 11448997]
47. Salhia B, Rutten F, Nakada M, Beaudry C, Berens M, Kwan A, Rutka JT. Inhibition of Rho-kinase affects astrocytoma morphology, motility, and invasion through activation of Rac1. Cancer research. 2005; 65:8792–8800. [PubMed: 16204049]
48. Cox EA, Sastry SK, Huttenlocher A. Integrin-mediated adhesion regulates cell polarity and membrane protrusion through the Rho family of GTPases. Mol Biol Cell. 2001; 12:265–277. [PubMed: 11179414]
49. Kaverina I, Krylyshkina O, Small JV. Regulation of substrate adhesion dynamics during cell motility. Int J Biochem Cell Biol. 2002; 34:746–761. [PubMed: 11950592]

50. Pankov R, Endo Y, Even-Ram S, Araki M, Clark K, Cukierman E, Matsumoto K, Yamada KM. A Rac switch regulates random versus directionally persistent cell migration. The Journal of cell biology. 2005; 170:793–802. [PubMed: 16129786]
51. Chang F, Lemmon CA, Park D, Romer LH. FAK Potentiates Rac1 Activation and Localization to Matrix Adhesion Sites: A Role for betaPIX. Mol Biol Cell. 2007; 18:253–264. [PubMed: 17093062]
52. Ren XD, Kiosses WB, Sieg DJ, Otey CA, Schlaepfer DD, Schwartz MA. Focal adhesion kinase suppresses Rho activity to promote focal adhesion turnover. Journal of cell science. 2000; 113(Pt 20):3673–3678. [PubMed: 11017882]
53. Sander EE, ten Klooster JP, van Delft S, van der Kammen RA, Collard JG. Rac downregulates Rho activity: reciprocal balance between both GTPases determines cellular morphology and migratory behavior. The Journal of cell biology. 1999; 147:1009–1022. [PubMed: 10579721]
54. Nimnual AS, Taylor LJ, Bar-Sagi D. Redox-dependent downregulation of Rho by Rac. Nature cell biology. 2003; 5:236–241.
55. Ohta Y, Hartwig JH, Stossel TP. FilGAP, a Rho- and ROCK-regulated GAP for Rac binds filamin A to control actin remodelling. Nature cell biology. 2006; 8:803–814.
56. Tsuji T, Ishizaki T, Okamoto M, Higashida C, Kimura K, Furuyashiki T, Arakawa Y, Birge RB, Nakamoto T, Hirai H, Narumiya S. ROCK and mDia1 antagonize in Rho-dependent Rac activation in Swiss 3T3 fibroblasts. The Journal of cell biology. 2002; 157:819–830. [PubMed: 12021256]
57. Yip SC, El-Sibai M, Coniglio SJ, Mouneimne G, Eddy RJ, Drees BE, Neilsen PO, Goswami S, Symons M, Condeelis JS, Backer JM. The distinct roles of Ras and Rac in PI 3-kinase-dependent protrusion during EGF-stimulated cell migration. Journal of cell science. 2007; 120:3138–3146. [PubMed: 17698922]

Highlights

- This study, for the first time, describes a tumor suppressor needed for cancer cell motility
- The study reconciles many reports showing contradictory roles of RhoA in cell motility
- The study highlights the importance of the regulation of RhoA activity in astrocytoma cell motility
- The study establishes StarD13 as a GAP playing a major role in this process.

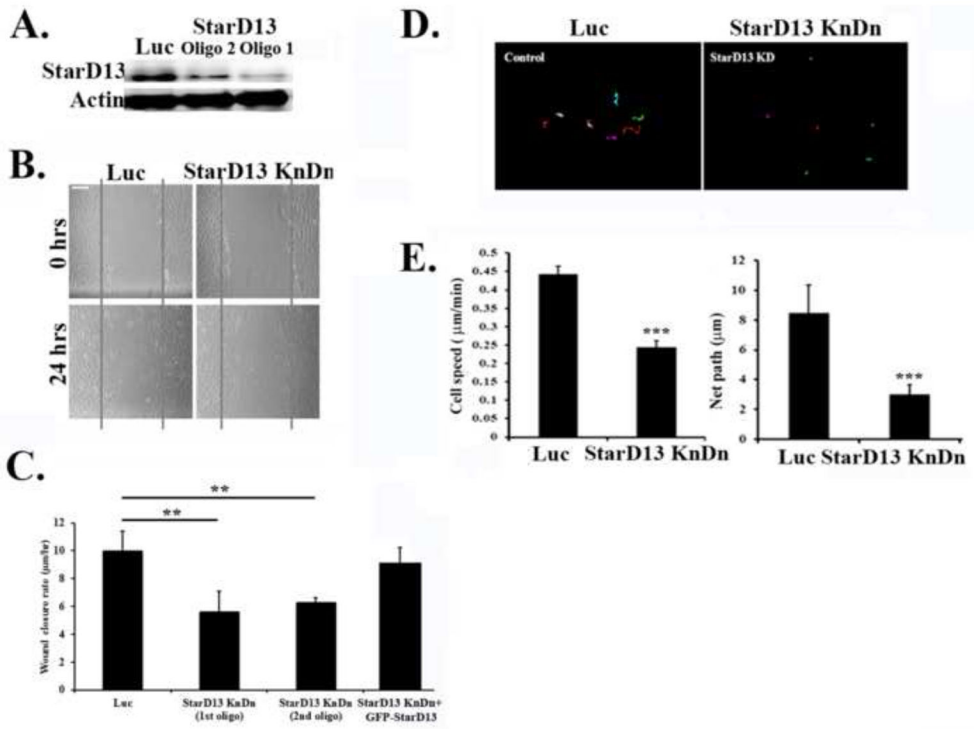

Figure 1. StarD13 is needed for cell motility

Cells (T98G) were transfected with luciferase control siRNA or with StarD13 siRNA (2 oligos) for 72 hours. **A)** The cells were lysed and immunoblotted by western blot analysis for StarD13 (upper gel) or for actin (lower gel) for loading control. **B)** Cells transfected with luciferase siRNA, StarD13 siRNA, or StarD13 siRNA and GFP-StarD13 were grown in a monolayer then wounded and left to recover the wound then imaged at the same frame after 24 hours (lower micrographs). Scale bar is 50 μm. **C)** Quantitation for B). Wound widths were measured at 11 different points for each wound, and the average rate of wound closure for the cells was calculated in μm/hr. Data are the mean −/+ SEM from 3 wound closure movies. ** indicates that the value is significant with $p<0.01$. **D)** The net paths of projected 120 frames from 2 hour long time lapse movies of cells (SF268) transfected with luciferase control siRNA or with StarD13 siRNA undergoing random motility in serum (different colors represent different cells) **E)** Quantitation of the cell speed from D) expressed in μm/min or the net paths shown expressed in μm. Data are the mean −/+ SEM from 15 cells. *** indicates that the values are significant with $p<0.001$.

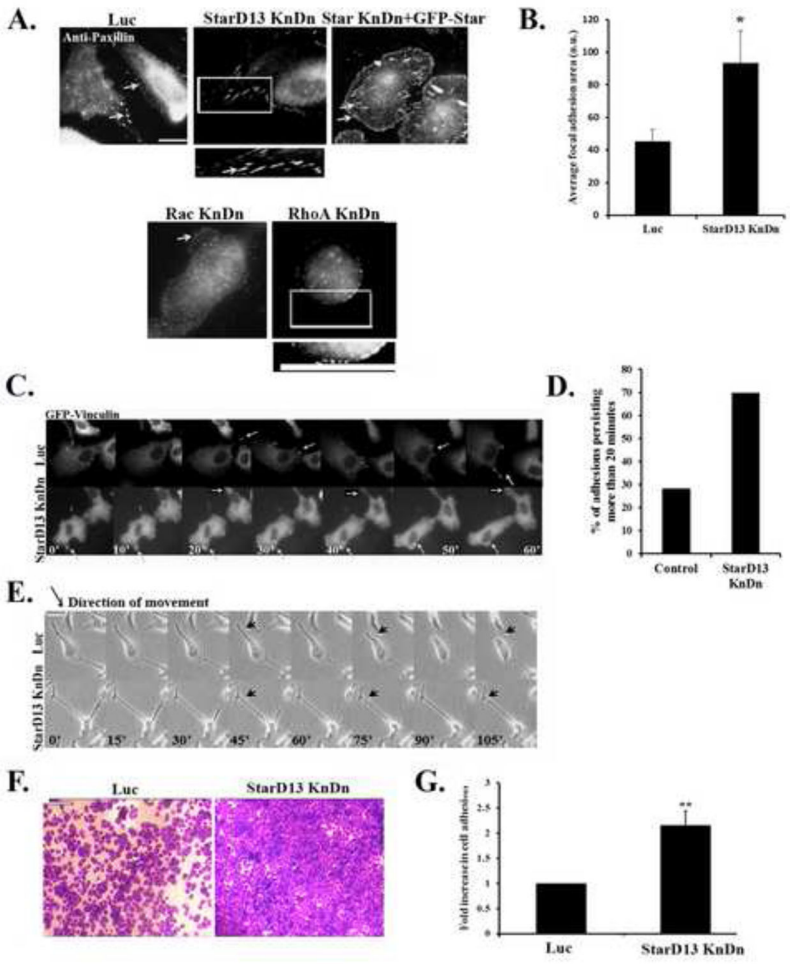

Figure 2. Proper regulation by StarD13 of Rho GTPases is needed for adhesion dynamics and tail detachment

A) Representative micrographs of cells (T98G) transfected with luciferase control, StarD13 siRNA or StarD13 siRNA and GFP-StarD13 (upper panel) or RhoA and Rac siRNA (lower panel) that were fixed and immunostained with paxillin. **B)** Quantitation of focal adhesion size in cells transfected with luciferase control or StarD13 siRNA. Data are the mean +/− SEM from 3 different experiments. **C)** Representative fluorescent micrographs taken from a time lapse of cells were transfected with luciferase or StarD13 siRNA and then transfected with GFP-vinculin and imaged while undergoing random motility in serum for 1 hour. **D)** Quantitation of C) showing percentage of focal adhesions persisting more than 20 minutes (Control n=32 and StarD13 siRNA n=23). **E)** Representative phase contrast micrographs taken from a time lapse of cells were transfected with luciferase or StarD13 siRNA and imaged while undergoing random motility in serum for 2 hours. **F)** Representative micrographs of cells fixed and stained with crystal violet to detect adhesion (as described in methods). Scale bar is 50 μm. **G)** Graph shows quantitation of F) where crystal violet was solubilized and the absorption of the plates was read at 550 nm using an ELISA plate reader. Data is measured in arbitrary units and normalized to the luciferase control. Data are the

mean −/+ SEM from 3 experiments (15 cells/condition/experiment). ** indicates that the value is significant with p=0.007.

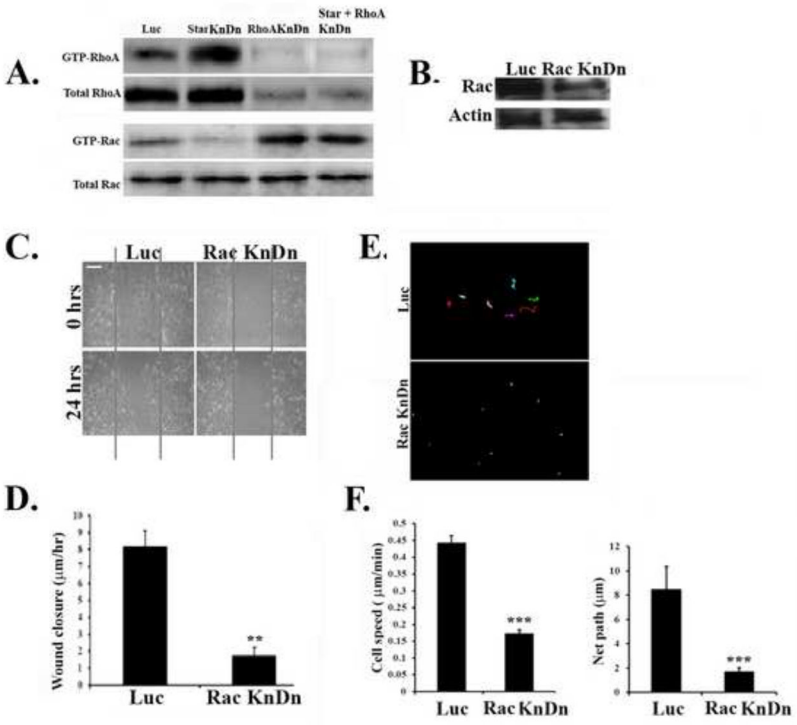

Figure 3. Effect of StarD13-RhoA on Rac activation which is needed for cell motility

A) T98G cells were transfected with luciferase, StarD13, RhoA, or StarD13 and RhoA siRNA for 72 hours. The cells were then lysed and incubated with GST-RBD (Rhotekin binding domain), or with GST-CRIB (Cdc42 and Rac interactive binding domain) to pull down active RhoA or Rac respectively. The samples were then blotted with RhoA or Rac antibody. The lower gel in each panel is a western blot for the total cell lysates for loading control. **B)** Cells (T98G) were transfected with luciferase control siRNA or with Rac siRNA for 72 hours. The cells were lysed and immunoblotted by western blot analysis for Rac (upper gel) or for actin (lower gel) for loading control. **C)** The luciferase siRNA-transfected and Rac siRNA-transfected cells were grown in a monolayer then wounded and left to recover the wound then imaged at the same frame after 24 hours (lower micrographs). Scale bar is 50 μm. **D)** Quantitation for C). Wound widths were measured at 11 different points for each wound, and the average rate of wound closure for the cells was calculated in μm/hr. Data are the mean −/+ SEM from 3 wound closure movies. ** indicates that the value is significant with p=0.001. **E)** The net paths of projected 120 frames from 2 hour long time lapse movies of cells (SF268) transfected with luciferase control siRNA or with Rac siRNA undergoing random motility in serum (different colors represent different cells) **F)** Quantitation of the cell speed from F) expressed in μm/min or the net paths shown expressed in μm. Data are the mean −/+ SEM from 15 cells. *** indicates that the values are significant with $p<0.001$.

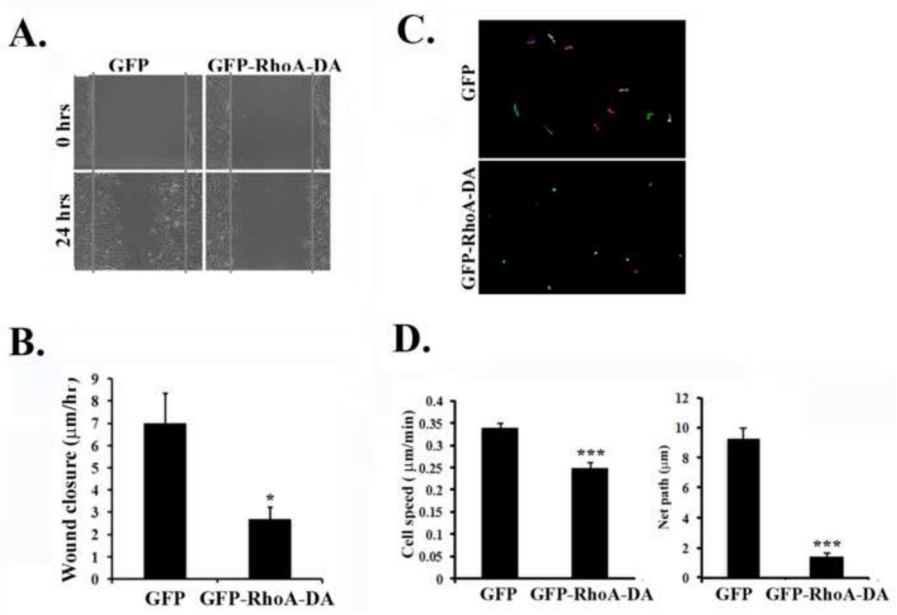

Figure 4. Constitutively active RhoA inhibits cell motility

A) Cells (T98G) were transfected with GFP vector or dominant active RhoA construct (RhoA DA). Cells were grown in a monolayer then wounded and left to recover the wound then imaged at the same frame after 24 hours (lower micrographs). **B)** Quantitation for A). Wound widths were measured at 11 different points for each wound, and the average rate of wound closure was calculated in μm/hr. Data are the mean −/+ SEM from 3 wound closure movies. * indicates that the value is significant with p=0.01. **C)** Cells (SF268) were transfected with GFP vector or with GFP-RhoA-DA. The images show net paths of projected 120 frames from 2 hour long time lapse movies of green cells undergoing random motility in serum (different colors represent different cells). **D)** Quantitation of the cell speed from D) expressed in μm/min or the net paths shown expressed in μm. Data are the mean −/+ SEM from 15 cells. *** indicates that the values are significant with p<0.001.

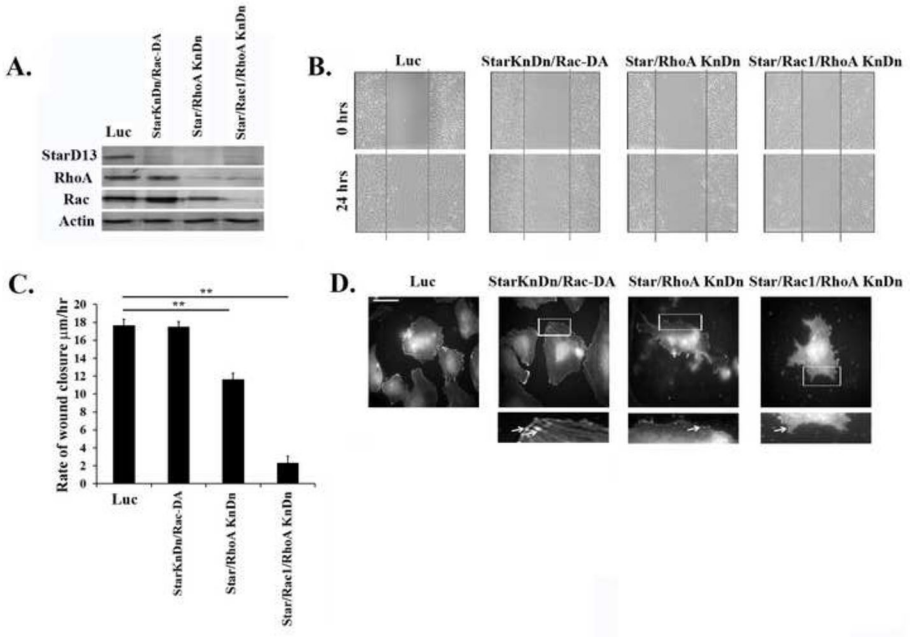

Figure 5. StarD13 regulation of focal adhesions is needed for cell motility

A) Cells were transfected with luciferase control, StarD13 and dominant active Rac, StarD13 and RhoA siRNA, or StarD13, Rac, and RhoA siRNA, lysed and western blots of total lysates blotted with StarD13, RhoA, Rac or actin antibodies. **B)** Same cells as in A) transfected and grown in a monolayer then wounded and left to recover the wound then imaged at the same frame after 24 hours (lower micrographs). **C)** Quantitation for B). Wound widths were measured at 11 different points for each wound, and the average rate of wound closure for the cells was calculated in μm/hr. Data are the mean −/+ SEM from 3 wound closure movies. ** indicates that the values are significant with $p<0.01$. **D)** Representative micrographs of cells (T98G) transfected with luciferase control, StarD13 and Rac siRNA, StarD13 and RhoA siRNA, or StarD13, Rac, and RhoA siRNA that were fixed and immunostained with paxillin. Scale bar is 10 μm.

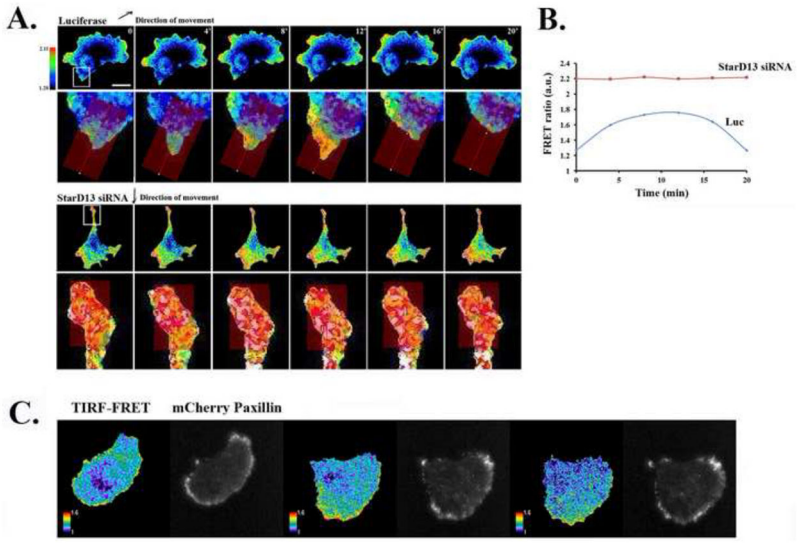

Figure 6. StarD13 knockdown inhibits cycling of RhoA activity and RhoA actication co-localizes with focal adhesions

A) Montage of representative SF268 cells (15 cells/condition/experiment of 3 experiments) transfected with luciferase or StarD13 siRNA and with the RhoA FRET biosensor undergoing motility in serum with the direction of migration indicated by an arrow (frames are 4 min apart). The lower panels for each cell types are a closeup of the area enclosed by a white box in the upper panels. **B)** The graph is a quantitation of the FRET signal in the area indicated by the shadowed area in the lower panels representing the cell tail. **C)** SF268 cells were transfected with 500ng of the RhoA biosensor plasmid and 500ng of the mCherry-Paxillin plasmid. The paxillin signal and the FRET signal were collected on a TIRF station.

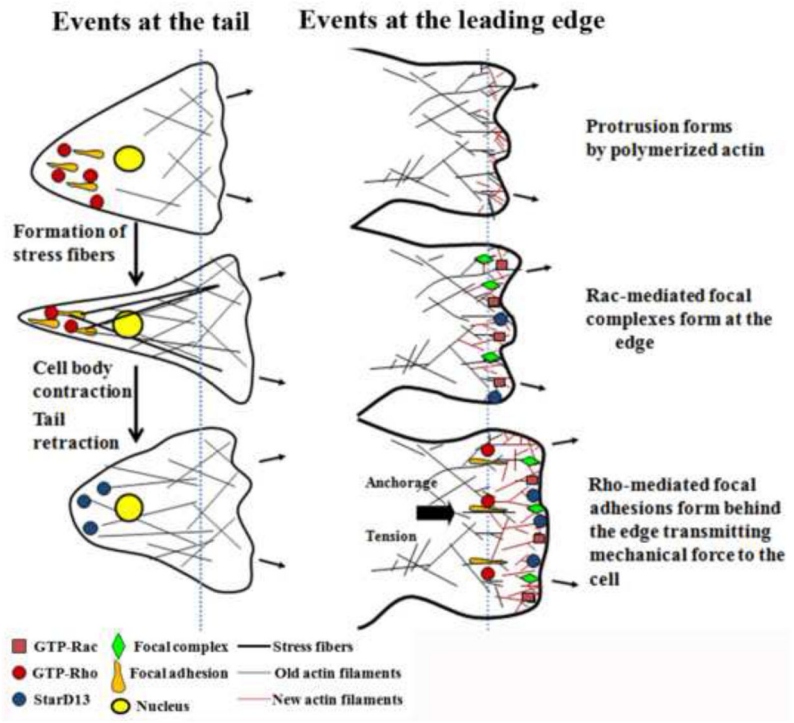

Figure 7.

Model of StarD13 regulation of RhoA activation at the tail and at the leading edge of astrocytoma cells undergoing cell motility.